G protein signaling–biased mu opioid receptor agonists that produce sustained G protein activation are noncompetitive agonists

Edward L. Stahl[a], Cullen L. Schmid[a], Agnes Acevedo-Canabal[a], Cai Read[a], Travis W. Grim[a], Nicole M. Kennedy[a], Thomas D. Bannister[a], and Laura M. Bohn[a,1]

[a]Department of Molecular Medicine, Scripps Research, Jupiter, FL 33458

Edited by Robert J. Lefkowitz, HHMI, Durham, NC, and approved October 22, 2021 (received for review February 5, 2021)

The ability of a ligand to preferentially promote engagement of one signaling pathway over another downstream of GPCR activation has been referred to as signaling bias, functional selectivity, and biased agonism. The presentation of ligand bias reflects selectivity between active states of the receptor, which may result in the display of preferential engagement with one signaling pathway over another. In this study, we provide evidence that the G protein–biased mu opioid receptor (MOR) agonists SR-17018 and SR-14968 stabilize the MOR in a wash-resistant yet antagonist-reversible G protein–signaling state. Furthermore, we demonstrate that these structurally related biased agonists are noncompetitive for radiolabeled MOR antagonist binding, and while they stimulate G protein signaling in mouse brains, partial agonists of this class do not compete with full agonist activation. Importantly, opioid antagonists can readily reverse their effects in vivo. Given that chronic treatment with SR-17018 does not lead to tolerance in several mouse pain models, this feature may be desirable for the development of long-lasting opioid analgesics that remain sensitive to antagonist reversal of respiratory suppression.

biased agonism | tolerance | naloxone | efficacy | allostery

Opioids such as morphine bind to the mu opioid receptor (MOR) and couple to inhibitory Gα ($G\alpha_i$) proteins to promote opioid-induced analgesia (1). Upon chronic exposure, the MOR is phosphorylated by GPCR kinases and binds to β-arrestins, a process that contributes to MOR desensitization (2–5). In mice, genetic perturbation of these regulatory events has been shown to attenuate morphine tolerance (6–9); therefore, agonists that activate MOR but do not lead to β-arrestin2 recruitment have been pursued to provide analgesia without tolerance (10). Agonists that display functional selectivity for promoting receptor interactions with certain signaling pathways over others are frequently described as biased agonists. This concept of functional selectivity suggests that the receptor may assume more than one active state, thereby permitting pleiotropic signal propagation (11–16). Recently, we described a series of compounds that have varying degrees of signaling bias and intrinsic efficacy that include: partial agonists promoting a preference for recruiting β-arrestin2 over G protein signaling (fentanyl and SR-11501); partial agonists promoting a G protein signaling preference (SR-17018, SR-15098, and SR-15099); and full agonists inducing G protein signaling preference (SR-14968) (17).

These agonists produce antinociception in mice; moreover, the G protein signaling–biased agonists display an improvement in the therapeutic window (respiratory suppression ED_{50} over antinociception ED_{50}) that is directly proportional to the degree of signaling bias observed (17). Interestingly, chronic treatment of mice with SR-17018 does not produce tolerance in the hot plate assay, the formalin pain test, nor or a chemotherapeutic-induced neuropathic pain model (18). These observations support the hypothesis that extended treatment with certain types of G protein–biased MOR agonist may present a means to limit the development of antinociceptive tolerance (7, 9, 19–21). While the development of opioid tolerance is likely more complex than simply the desensitization of the receptor, chronic morphine treatment does lead to a decrease in agonist-stimulated ^{35}S-GTPγS binding in mouse brain membranes compared to saline-treated mice (9, 22–25) suggesting that desensitization of MOR-G protein signaling may contribute to antinociceptive tolerance.

In cell culture, MOR desensitization can be modeled by pretreatment of cells with opioid agonists, which leads to decreased sensitivity upon subsequent agonist exposure in G protein signaling assays (1, 2, 24). In this study, we ask whether agonists that are less likely to induce β-arrestin2 recruitment will be less likely to induce receptor desensitization using this conventional model. Pretreatment of cells with G protein signaling–biased agonists (described in ref. 17) leads to a wash-resistant elevation in basal GTPγS binding that is reversible by antagonist. Interestingly, these properties are not observed for the structurally related β-arrestin2–biased agonist SR-11501 nor the G protein–biased agonist of a different structural class: oliceridine. Evaluation in mouse brainstem membranes further supports the noncompetitive nature of the MOR-biased agonists from the SR series. Importantly, we demonstrate that that while SR-14968 is noncompetitive with naloxone in biochemical studies; a low dose of naloxone can fully reverse SR-14968-induced respiratory suppression in mice. Overall, these findings speak to the complexity that underlies the manifestation of

Significance

Analgesic tolerance can result upon chronic use of opioid drugs necessitating dose escalation to treat pain. The biased mu opioid receptor agonist SR-17018 maintains antinociceptive efficacy without evidence of tolerance when given chronically to mice. Here, we show that SR-17018 and related compounds are noncompetitive agonists that stabilize the receptor in an active state that can still be blocked by orthosteric antagonists. We propose that this mode of activation may contribute to the biased agonists' apparent ability to preferentially induce G protein signaling in cellular assays and may underlie the enduring efficacy observed for SR-17018 in vivo.

Author contributions: E.L.S., C.L.S., A.A.-C., and L.M.B. designed research; E.L.S., C.L.S., A.A.-C., C.R., and T.W.G. performed research; N.M.K. and T.D.B. contributed new reagents/analytic tools; E.L.S., C.L.S., A.A.-C., C.R., and L.M.B. analyzed data; E.L.S. and L.M.B. wrote the paper; and T.D.B. supervised chemistry.

Competing interest statement: The Scripps Research Institute has filed for a patent on the SR compounds used in this study.

This article is a PNAS Direct Submission.

[1]To whom correspondence may be addressed. Email: lbohn@scripps.edu.

This article contains supporting information online at http://www.pnas.org/lookup/suppl/doi:10.1073/pnas.2102178118/-/DCSupplemental.

Published November 24, 2021.

apparent signaling bias observed for different agonists at MOR and may point to properties that will be desirable for avoiding MOR adaptations underlying desensitization and antinociceptive tolerance.

Results

Increased Baseline Signaling Following Exposure to Biased Agonists. A 2 h pretreatment (10 μM) of human MOR–CHO (Chinese hamster ovary) cells with morphine, fentanyl, oliceridine, and SR-11501 results in MOR desensitization, which is evident by a decrease in DAMGO ([D-Ala_2, *N*-Me-Phe_4, Gly_5-ol-Enkephalin], and trifluoroacetate salt) potency and efficacy relative to the parameters obtained following vehicle pretreatment (Fig. 1*A* and Table 1). Interestingly, pretreatment with SR-17018 and SR-14968 raises basal ^{35}S-GTPγS binding despite extensive washing of the cells and the membranes. SR-15098 and SR-15099, two agonists that are structurally related to SR-17018 (17), also increase basal GTPγS binding (Fig. 1*B*). This increased basal activity can be observed following a shorter incubation period (30 min) with SR-17018 and SR-14968, and no increase in GTPγS binding was observed following pretreatment in untransfected CHO cells indicating that the effect is receptor-mediated (*SI Appendix*, Fig. 1).

While MOR activation leads to the inhibition of adenylyl cyclase, chronic treatment with MOR agonists sensitizes adenylyl cyclase activity resulting in a forskolin-induced "overshoot" in cyclic adenosine monophosphate (cAMP) production (26, 27). As shown in Fig. 1*C*, pretreatment with morphine (10 μM, 2 h) produces the anticipated sensitization to forskolin-stimulated cAMP accumulation compared to vehicle. By contrast, pretreatment with SR-17018 does not induce this overshoot; rather, forskolin-stimulated cAMP accumulation is decreased compared to the vehicle-treated cells, suggesting that SR–17018 remains bound to MOR and that the receptor remains actively engaged in inhibitory $G\alpha_i$ signaling.

SR-17018 and SR-14968 pretreatment leads to dose-dependent increases in basal GTPγS binding (Fig. 1 *D* and *E*). DAMGO is able to further activate MOR in the CHO cells following SR-17018 pretreatment, although the potency of DAMGO is shifted rightward after the 10 μM pretreatment (Table 1 and Fig. 1*F*). In addition to raising the baseline, pretreatment with the full agonist SR-14968 decreases the maximum response produced by DAMGO to the point at which the system loses the capacity to respond to DAMGO (Fig. 1*G* and Table 1). Fig. 1*H* compares the concentration-dependent stimulation of GTPγS binding following "acute" application of SR-17018 to the MOR–CHO cells to the remaining "residual" stimulation observed following the 2 h SR-17018 pretreatment. The acute and residual response produced by SR-17018 reaches an equivalent maximum suggesting both a lack of significant SR-17018 dissociation and a conserved level of maximum agonist activity (because the maximum response of partial agonists is produced at full occupancy). A similar comparison is made for SR-14968 (Fig. 1*I*). Here, the residual stimulation plateaus at ∼50% of the maximum stimulation induced by SR-14968 in the acute treatment. Together, these data suggest that SR-17018 and SR-14968 may be acting as irreversible agonists. Strikingly, these effects are readily reversed by the MOR antagonists, naloxone, and CTOP (Fig. 1 *J* and *K* and Table 1). These observations suggest that the compounds are binding tightly to a different site than the conventional antagonists; their agonism persists despite extensive washing, but the activity they produce can still be inhibited by a competitive antagonist.

Preservation of Increased Basal Activity in Intact Cells and Isolated Membranes. Pretreatment of live MOR–CHO cells with 10 μM morphine, fentanyl, SR-11501, and SR-17018 leads to a moderate decrease in ^{3}H-naloxone (5 nM) binding in intact cells (Fig. 2*A*). The 10 μM pretreatment with SR-14968 nearly abolishes all detectable ^{3}H-naloxone binding; moreover, this effect is concentration dependent (Fig. 2*B*). A loss of radioligand binding sites may indicate a loss of receptor at the cell surface as has been previously shown for many of the compounds used in this study (28). Therefore, to avoid cellular adaptations that may occur in response to extended drug exposure (i.e., internalization and down-regulation), isolated MOR–CHO cell membranes were pretreated for 30 min followed by extensive washes. Again, pretreatment results in a decrease in ^{3}H-naloxone binding (Fig. 2*C*) suggesting that the loss of naloxone binding is not due to the removal of accessible receptors.

A 10- or 30-min pretreatment of prepared membranes is also sufficient to elevate GTPγS basal activity with SR-17018 and SR-14968, further demonstrating that an intact cell is not required for this sustained activation to occur (Fig. 2 *D* and *E*). The increased basal GTPγS binding in the pretreated membranes can also be reversed by an antagonist (Fig. 2*E*) as in intact cells (Fig. 1*J*) suggesting that the antagonists still have access to the orthosteric pocket in the presence of residual agonist activation. We further interrogated the nature of the SR-17018 interaction with MOR by exploring the contribution of sodium to its activity. Sodium ions have been shown to allosterically modulate MOR to decrease constitutive activity (29–33) allowing agonist activity to be revealed (34, 35). In vehicle-pretreated MOR–CHO membranes prepared in the absence of sodium, basal activity is high, and no effect of DAMGO is observed; as NaCl is added back, the baseline GTPγS binding decreases, and DAMGO-mediated stimulation is revealed (Fig. 2*F*, and as previously shown in seminal studies, refs. 34 and 35). Notably, 100 mM NaCl is the standard concentration used throughout this study in which optimal agonism is observed. In the SR-17018-pretreated cells, the basal GTPγS binding level is similar to the vehicle-pretreated cells in the absence of NaCl; however, increasing the concentration of NaCl has no effect on the basal GTPγS binding suggesting that the SR-17018 pretreatment induces an active state that is no longer negatively regulated by sodium ions.

SR-17018 and SR-14968 pretreatment also increases basal GTPγS binding in membranes from CHO cells expressing the mouse MOR (Fig. 2*G*) demonstrating that the effect is not unique to the human MOR. Only SR-14968 produces a significant elevation of GTPγS binding in mouse brainstem membranes following a 30-min pretreatment, which may be due to the heterogeneity of this system. Importantly, brainstem membranes prepared from MOR knockout (MOR-KO) mice have no response to the agonists (Fig. 2*H*). Baselines are also elevated following pretreatment of membranes from the human neuroblastoma cell line SHSY-5Y, wherein MOR is endogenously expressed (Fig. 2*I*). Together, these data indicate that the stabilization of the G protein signaling state occurs independently of receptor trafficking, can occur in endogenous tissues, and is not an artifact of an overexpression system.

Competitive Analysis of Agonist Activity in the Presence of Naloxone. Naloxone decreases the potency of DAMGO in a linear dose-dependent fashion as would be expected by a competitive interaction between two orthosteric ligands (Fig. 3*A*). Naloxone dose-dependently shifts the potency of SR-17018 as well. However, due to the partial agonism and modest potency of SR-17018, it is difficult to accurately define the top of the curve at higher concentrations of naloxone (Fig. 3*B*). We do observe a linear rightward shift in the SR-17018 response curves in the presence of naloxone as would be expected if the two ligands act competitively (Fig. 3*B*). The naloxone inhibition of SR-14968 also produces a linear rightward shift in the potency;

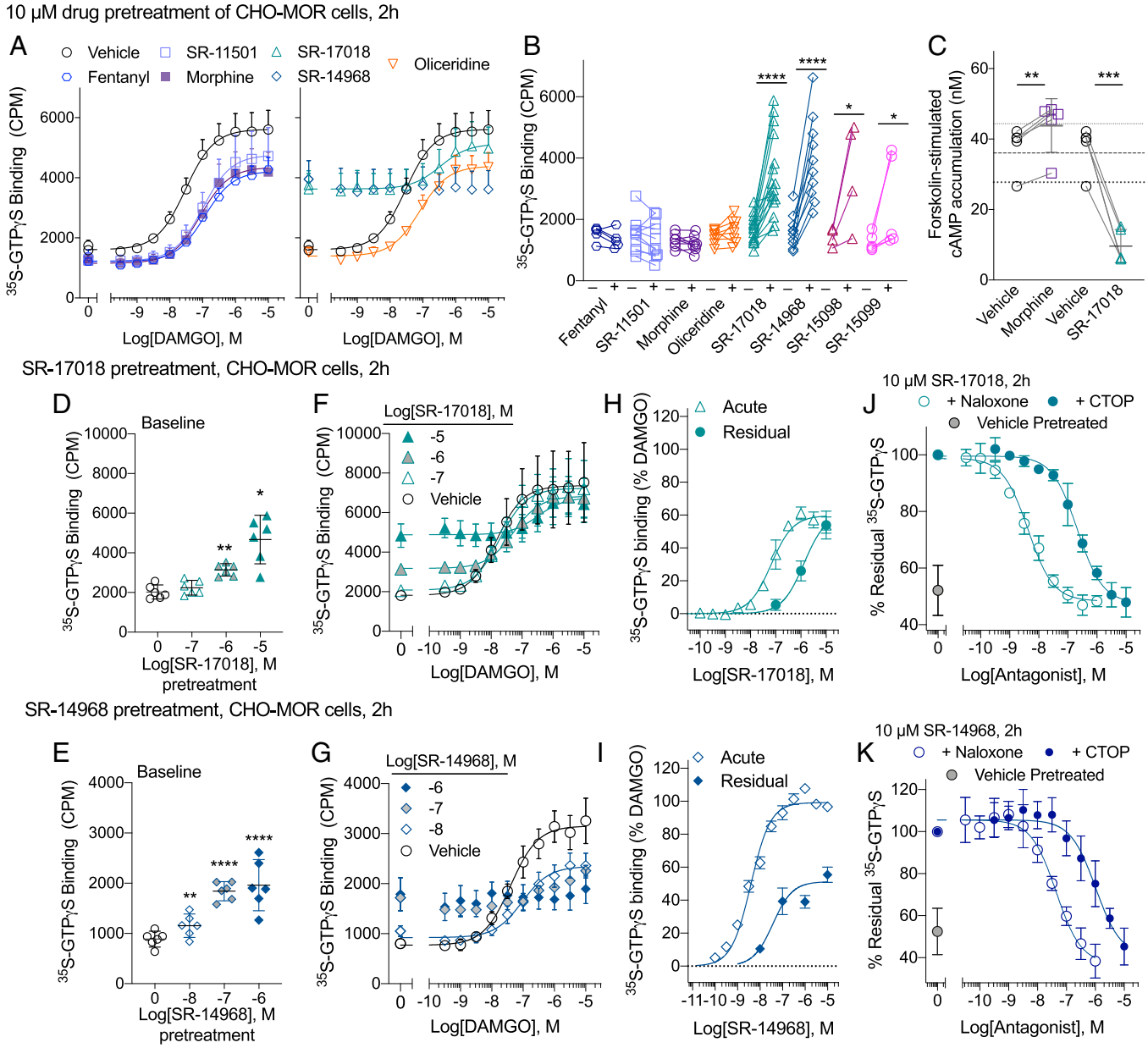

Fig. 1. Pretreatment of live MOR–CHO cells with SR-14968 and SR-17018 increase wash-resistant, antagonist-reversible, basal G protein activation following extended exposure. (*A*) DAMGO-stimulated ^{35}S-GTPγS binding following a 2-h, 10-μM treatment with indicated agonists (n = 5 to 7 per compound, 16 vehicle, mean ± SEM plotted). (*B*) Individual baseline values following indicated agonist or corresponding vehicle pretreatment tested in parallel (10 μM, 2 h, n = 4 to 16). (*C*) Morphine (10 μM, 2 h) pretreatment enhances forskolin-induced cAMP production, while SR-17018 pretreatment (10 μM, 2 h) suppresses the cAMP accumulation (n = 3). (*D*) The dose-dependent increase of basal GTPγS binding following SR-17018 and (*E*) SR-14968 2 h pretreatment [mean with 95% CI plotted, n = 6, which includes n = 3 and the individual baseline points for *F* (n = 3) and *G* (n = 3)]; (*F*) DAMGO activation following SR-17018 pretreatment (n = 3) and (*G*) SR-14968 pretreatment (n = 3). (*H*) A comparison of an acute concentration response curve of SR-17018 (n = 3) or (*I*) SR-14968 (n = 3) to the residual basal activity produced by a 2-h pretreatment at the concentrations indicated (plotted from *F* and *G*). (*J*) A naloxone and CTOP antagonism of the residual elevated baseline produced by a 2-h, 10-μM pretreatment of SR-17018 (n = 3) or (*K*) SR-14968 (n = 3). Statistical differences are indicated relative to vehicle pretreatment performed in parallel as *P < 0.05; **P < 0.01; ****P < 0.0001; paired Student's t test. See Table 1.

however, the maximum response is clearly decreased in the presence of naloxone (Fig. 3*C*). This effect is most likely the product of a noncompetitive inhibition as DAMGO is capable of surmounting naloxone inhibition as shown in Fig. 3*A*. Fitting the data in Fig. 3*C* to the allosteric operational model which permits allosteric modulation of both affinity and efficacy when both sites of the receptor are occupied, produces an αβ value of 0.0029 (Table 2, in which α defines the potency shift and β defines the change in magnitude produced by an allosteric interaction between two ligands).

Competitive Mechanisms Assessed by Radioligand Competition Binding. All of the agonists fully inhibit ^{3}H-DAMGO binding and give no indication of a noncompetitive interaction, which is in agreement with the report of their binding affinities using ^{3}H-DAMGO shown in Fig. 3*D* (17). Interestingly, the G protein signaling–biased agonists, which elevate baseline GTPγS binding upon extended exposure (Fig. 1*B*) only partially block binding of the high affinity radioligand ^{3}H-diprenorphine (Fig. 3*E*). Partial inhibition was also observed using SR-17018 and SR-14968 in ^{3}H-naloxone–binding assays; interestingly, the addition of SR-17018

Table 1. Changes in potencies and efficacies following pretreatment of live cells for 2 h with indicated opioid agonists

Figure	2 h Pretreatment	DAMGO EC_{50}, nM	DAMGO %Emax	Figure	2 h Pretreatment	DAMGO EC_{50}, nM	DAMGO %Emax
1*A*	Vehicle	34 ± 14	100	1G	Vehicle	40 ± 14	100
	10 μM fentanyl	109 ± 36*	84 ± 25		0.01 μM SR-14968	84 ± 10	67 ± 13§
	10 μM SR-11501	106 ± 38*	71 ± 14*		0.1μM SR-14968	NC	[65 ± 11]
	10 μM morphine	87 ± 22†	74 ± 40		1 μM SR-14968	NC	[44 ± 3]
	10 μM oliceridine	80 ± 34†	90 ± 24			Naloxone IC_{50}, nM	CTOP IC_{50}, nM
	10 μM SR-17018	342 ± 162†	88 ± 26	1J	10 μM SR-17018	4.35 ± 0.59	224 ± 129
	10 μM SR-14968	NC	[48 ± 8]	1K	10 μM SR-14968	46 ± 8.2	1335 ± 884
1*F*	Vehicle	15 ± 6	100				
	0.1 μM SR-17018	19 ± 11	104 ± 26				
	1 μM SR-17018	57 ± 23	100 ± 28				
	10 μM SR-17018	278 ± 56‡	95 ± 21				

EC_{50} and E_{max} (mean ± SD), from the curves in Fig. 1 where [Emax] represents the maximum observed stimulation at 10 μM when the curve is not converged (NC). Fig. 1*A*: A paired Student's *t* test comparing vehicle and drug treatment within each group:
*$P < 0.01$;
†$P < 0.05$. ($n = 4$ to 6 per drug, 15 vehicles). Fig. 1*F*: SR-17018 versus vehicle: One-way RM-ANOVA= $F(1.175, 2.351) = 81.43$, $P = 0.0070$;
‡$P < 0.05$, Dunnett's post hoc analysis. n= 3. Fig. 1*G*: SR-14968 versus vehicle: paired Student's *t* test;
§$P < 0.05$ n= 3. Fig. 1 *J* and *K*: Means of the IC50 are presented with ± SD, $n = 3$ per set. Imax was not determined (ND) as there was no "baseline" in the drug pretreated samples. The average potency for all of the vehicle-pretreated groups (*A*–*G*): 32 ± 15 nM (SD, $n = 21$).

to SR-14968 increases ^{3}H-naloxone binding, suggesting that SR-14968 and SR-17018 are acting at a competitive allosteric site that is distinct from the ^{3}H-naloxone orthosteric site (Fig. 3*F*). For both ^{3}H-diprenorphine and ^{3}H-naloxone binding, partial inhibition is inconsistent with competitive orthosteric occupancy and is supported by a noncompetitive mechanism of action. Calculated pK_B and α parameters describing the allosteric interactions are provided in Table 3 along with potency parameters. These data strongly indicate that the selected biased agonists do not compete with the classic orthosteric site that diprenorphine/naloxone occupy in MOR.

Competitive Interactions Explored in Mouse Brainstem Membranes. A partial agonist will compete with a full agonist to decrease the maximal stimulation produced by the full agonist until it converges with the maximal response (efficacy) produced by the partial agonist alone (36). This relationship is exemplified in mouse brainstem membranes where the potent partial agonist sufentanil stimulates GTPγS binding to 31% maximum of DAMGO; in the presence of 1 μM DAMGO, sufentanil inhibits DAMGO down to sufentanil efficacy (32%) (Fig. 4*A* and Table 4 for parameters). This effect is recapitulated for SR-15011 and oliceridine (Fig. 4 *B* and *C*). Notably, oliceridine produces very little detectable stimulation in this assay (preventing the estimation of potency); however, the potency of oliceridine can be observed in the competition study in which it potently reverses 1 μM DAMGO stimulation down to the efficacy observed with oliceridine alone (Fig. 4*C*). By contrast, SR-15099 acts as a partial agonist relative to DAMGO in the brainstem GTPγS assay; however, the response observed with 1 μM DAMGO is not altered in the presence of increasing doses of SR-15099 (Fig. 4*D*). A similar effect can also be seen for the partial agonist SR-17018 (Fig. 4*E*). SR-14968 acts as a full agonist in mouse brainstems, and SR-17018, although incapable of inhibiting DAMGO stimulation, is capable of blocking SR-14968–mediated activation of MOR in the brainstem (Fig. 4*F*). Importantly, none of the agonists stimulate GTPγS binding in MOR-KO mouse brainstem membranes (*SI Appendix*, Fig. 2) (17). These observations further demonstrate that the SR series of G protein signaling–biased agonists are acting in a noncompetitive manner at MOR and do so in the mouse brain.

Reversal of SR-14968–Induced Respiratory Suppression by Naloxone. SR-14968 pretreatment greatly reduces the ability of low concentrations of ^{3}H-naloxone to bind in cell membranes, although naloxone is capable of completely inhibiting SR-14968–mediated G protein signaling (Figs. 1*K* and 2*B*). Therefore, we asked what this would mean for in vivo sensitivity to naloxone antagonism (Fig. 5). While SR-14968 has an improved therapeutic window (ED_{50} respiratory suppression: 14 mg/kg versus hot plate antinociception: 0.44 mg/kg) compared to fentanyl (ED_{50} respiratory suppression: 0.71 mg/kg versus hot plate antinociception: 0.24 mg/kg), SR-14968 still produces respiratory suppression in mice (17). Therefore, we tested if naloxone could block SR-14968-induced respiratory suppression. Based on the respiratory ED_{50} parameters previously determined, we compared equi-efficacious doses of SR-14968 and fentanyl. Fentanyl has a rapid onset and fast pharmacokinetic rate of clearance, while SR-14968 has a slower onset and is longer lasting (17). Therefore, naloxone was administered 15 min after fentanyl and 30 min after SR-14968. The reversal of fentanyl-induced respiratory suppression requires a relatively high dose of naloxone (37), and we show that 5 mg/kg naloxone is sufficient to reverse respiratory suppression produced by fentanyl at 1 mg/kg, intraperitoneally (i.p.) (Fig. 5*A*). Since the biochemical evidence indicates that naloxone is accessing a different site than SR-14968, we tested if a lower dose of naloxone could reverse the response produced by SR-14968. Remarkably, a 10-fold lower dose, 0.5 mg/kg, of naloxone fully reverses 10 mg/kg, i.p. SR-14968–induced respiratory suppression demonstrating that naloxone is highly efficacious against the noncompetitive agonist SR-14968 in vivo (Fig. 5*B*).

Discussion

In this study, we show that a series of G protein signaling–biased MOR agonists of a conserved chemical scaffold produce long-lasting and wash-resistant stimulation of GTPγS binding to membranes following a 10- to 120-min exposure. This activation is MOR-mediated, because it does not occur in untransfected cells. The studies suggest that SR-17018, SR-15099, and SR-14968 bind in a nearly irreversible manner to the MOR leading to persistent G protein signaling. However, the stimulation is fully reversed by the MOR antagonists, naloxone and CTOP, suggesting that the SR series compounds bind with high affinity to another site on the receptor that facilitates G protein signaling allowing the receptor to remain sensitive to antagonists that act at the orthosteric pocket. In both signaling and radioligand binding studies, we show that SR-17018 is capable of blocking the actions of SR-14968 suggesting that, while the compounds produce wash-

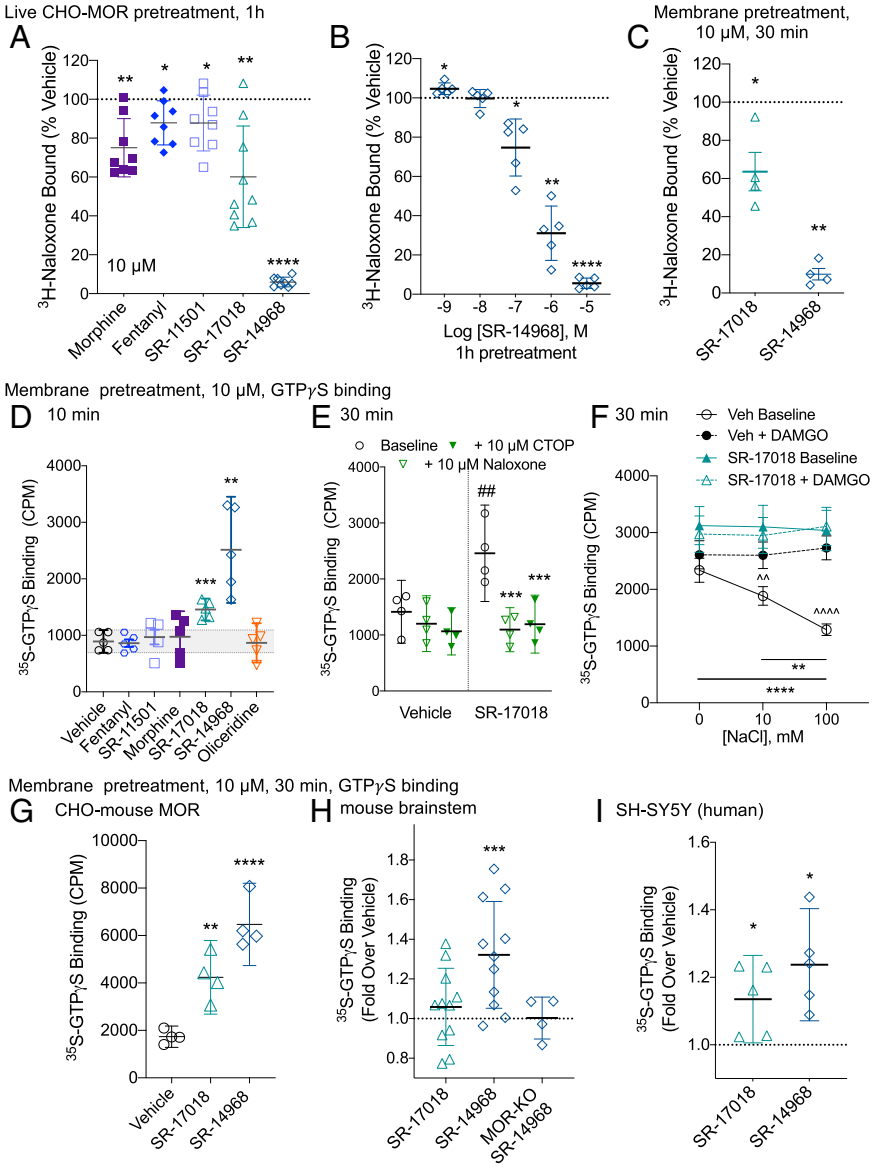

Fig. 2. The effects of SR-17018 and SR-14968 persist upon pretreatment of live cells or isolated membranes. (*A*) ^{3}H-Naloxone binding on whole MOR–CHO cells is decreased following 1-h pretreatment of live cells with 10 μM of the indicated compounds or (*B*) with indicated concentrations of SR-14968 compared to the vehicle. Pairwise analysis was made to a matched vehicle-pretreated in each experiment versus vehicle pretreatment raw values $*P < 0.05$; $**P < 0.01$; and $****P < 0.0001$ paired Student's *t* test, $n = 5$ to 9. (*C*) SR-17018 and SR-14968 (10 μM, 30 min) pretreatment of MOR–CHO membranes also decreases ^{3}H-naloxone binding (versus vehicle pretreatment raw values $*P < 0.05$ and $**P < 0.01$ paired Student's *t* test, $n = 4$). (*D*) Basal GTPγS binding is increased following a 10-min pretreatment of isolated membranes with 10 μM SR-17018 and SR-14968 (versus Vehicle pretreatment raw values $**P < 0.01$ and $***P < 0.001$). (*E*) The increased basal activity produced by a 10-μM, 30-min pretreatment with SR-17018 (versus vehicle pretreatment value $^{\#\#}P < 0.01$) is blocked by the acute application of 10 μM CTOP or Naloxone (versus SR-17018 and $***P < 0.001$, paired Student's *t* test). (*F*) The removal of NaCl results in an increased baseline that is evident in both SR-17018- and vehicle-pretreated membranes; the return of NaCl to the assay dose-dependently decreases basal activity only in the vehicle-pretreated cells (versus 0 mM NaCl: $**P < 0.01$ and $****P < 0.0001$); DAMGO-induced GTPγS binding is evident in the vehicle-pretreated membranes (versus DAMGO, $\wedge\wedge P < 0.01$, $\wedge\wedge\wedge\wedge P < 0.0001$, and one-way RM-ANOVA). No differences ($P > 0.05$) were observed under any conditions in the SR-17018-pretreated group. The mean with SEM presented, ($n = 6$). (*G–I*) Basal G protein signaling observed following a 30-min, 10-μM pretreatment of (*G*) CHO-mouse MOR membrane preparations ($n = 4$), (*H*) mouse brainstem membranes ($n = 11$) where MOR-KO brainstems served as a negative control ($n = 4$), and (*I*) SH-SY5Y cell membranes ($n = 5$). Due to greater variability in total radioactivity binding in the endogenous samples, the data are normalized to vehicle-pretreated levels run in parallel; paired Student's *t* test was performed comparing CPM values of agonist-pretreated to vehicle-pretreated; for *G* through *I*, versus vehicle-pretreated $*P < 0.05$; $**P < 0.01$; $***P < 0.001$; and $****P < 0.0001$; paired Student's *t* test.

resistant agonism, the two appear to be competitive for a shared and explicitly allosteric site. The persistent activity may be facilitated by the poor solubility of these agonists as they require dimethyl sulfoxide (DMSO) and detergent vehicles for administration in animals; moreover, given their high degree of brain penetrance (17, 25), they are expected to partition into membrane preparations, which likely contributes to the persistent G protein signaling observed despite extensive washing of the membranes. In this manner, these ligands may have additional access to sites on the receptor similar to models previously proposed for other receptors (38).

In this study, we have made every effort to present as much experimental data as possible in raw radioactivity counts (counts per minute [CPM]) to avoid misinterpretation due to normalization. If the data are normalized to fold over vehicle in Fig. 1, it would appear that SR-17018 and, to a greater extent, SR-14968 greatly desensitize the receptor following treatment as the baseline is greatly elevated. This profile has been observed previously using herkinorin, another agonist that was reported to have biased agonism at MOR (39, 40). In a similar desensitization study (40), MOR–CHO cells pretreated with herkinorin produced elevated basal GTPγS binding. Moreover, cAMP overshoot was suppressed following herkinorin treatment in a manner similar to that seen for SR-17018 (Fig. 1*C*). Molecular dynamic simulation and docking studies suggest that herkinorin interacts with N150$^{3.35}$ differently than classic MOR agonists (41); N150A$^{3.35}$ is predicted to interact directly with sodium ions which negatively regulate the active state of MOR (42). In the docking studies, the authors suggest that herkinorin is an allosteric modulator at MOR (41) but also propose occupancy in the orthosteric pocket. However, it has not been experimentally determined if herkinorin has noncompetitive interactions at MOR.

Since N150A$^{3.35}$ in MOR is involved in sodium ion binding (43), we investigated the contribution of sodium ions to the persistent elevated basal activity following SR-17018 pretreatment. Seminal studies demonstrated that agonist stimulation of GTPγS binding could only be observed in the presence of a monovalent cation such as sodium (as NaCl), which serves to decrease the basal degree of coupling enabling an agonist-induced receptor activation to be observed (34, 35). In vehicle-

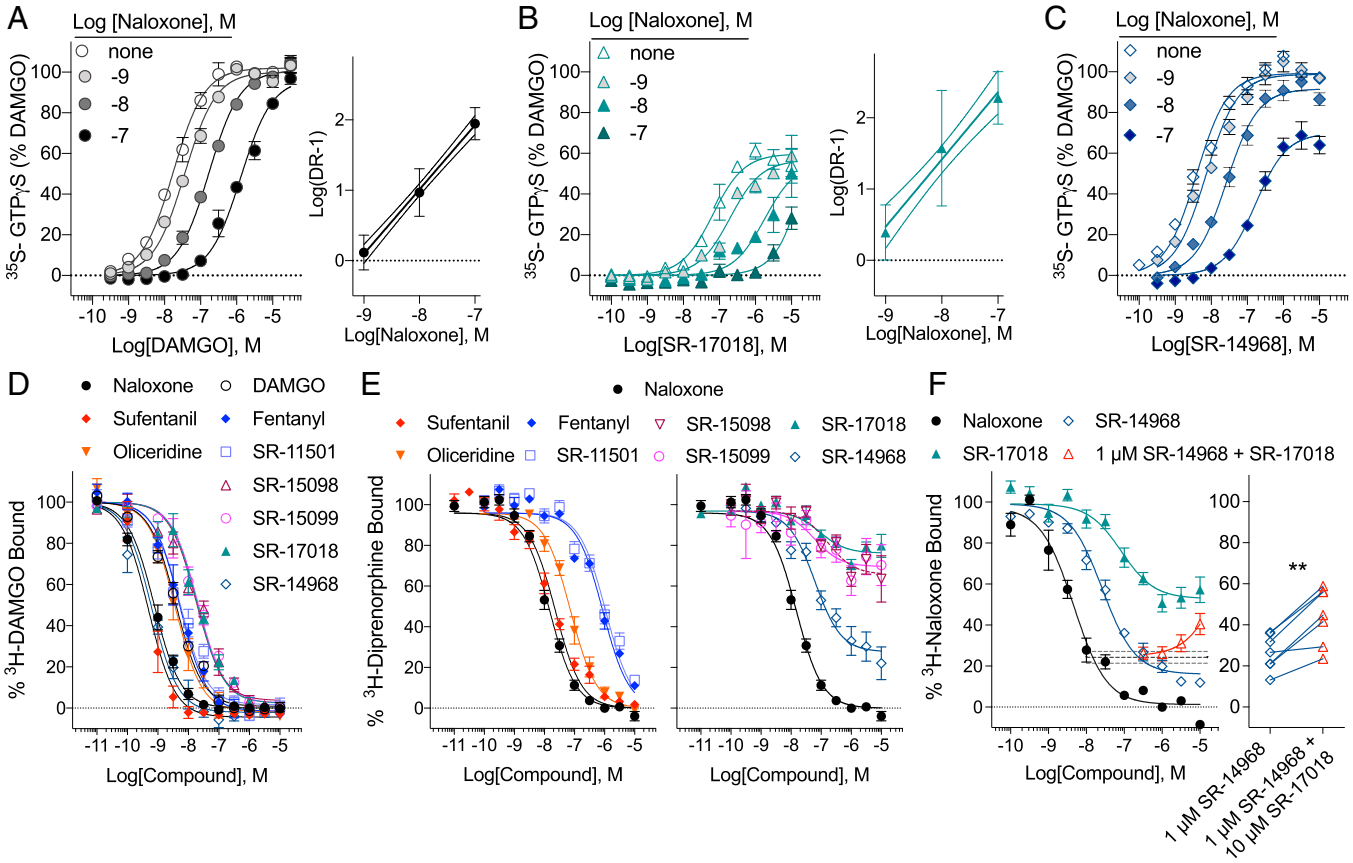

Fig. 3. SR-17018 and SR-14968 display noncompetitive interactions at MOR. (*A–C*) Competition curves in the ^{35}S-GTPγS binding assay on untreated MOR–CHO cell membranes are presented using increasing concentrations of naloxone in the presence of (*A*) DAMGO, (*B*) SR-17018, and (*C*) SR-14968 concentration response curves. Linear regression Schild analyses demonstrating a linear shift in the potency as a function of antagonist concentration are shown (n = 3). A decrease in the maximum of SR-14968 in the presence of 10 μM Naloxone is indicative of a noncompetitive interaction; the allosteric operational parameter αβ is calculated as 0.0029. (*D–F*) Radioligand competition studies using (*D*) ^{3}H-DAMGO, n = 3, (*E*) ^{3}H-Diprenorphine, n = 4 to 8, and (*F*) ^{3}H-Naloxone, n = 3, and the indicated competing compounds. The ^{3}H-naloxone competition produced by 1 μM SR-14968 (dashed line with SEM in *F*) can be reversed by SR-17018 (red triangles); the individual data points are shown for 10 μM SR-17018 (**P < 0.01, paired Student's t test). See Table 3 for parameters and n values.

pretreated membranes, we reproduced this experiment showing elevation of basal GTPγS binding in the absence of sodium, the decrease of basal GTPγS binding with increasing NaCl concentrations, and the subsequent restoration of agonist-stimulated MOR activation in the presence of sodium (34). However, following SR-17018 pretreatment, the basal GTPγS binding is not further elevated in the absence of sodium, and increasing NaCl levels does not decrease the basal activity (Fig. 2*F*). If SR-17018 is irreversibly binding in the orthosteric pocket, then it might be expected to prevent access to the sodium pocket. However, our studies demonstrate that SR-17018 is not an insurmountable agonist, as naloxone and CTOP (a larger, lower affinity peptide antagonist) readily block SR-17018 elevation of basal MOR signaling. Therefore, we propose that SR-17018 stabilizes the receptor in an active state that has low affinity for sodium binding.

In acute competition radioligand binding assays, the compounds appear to be fully competitive for ^{3}H-DAMGO binding, while the biased SR compounds do not fully displace ^{3}H-diprenorphine and ^{3}H-naloxone binding, suggesting a distinctly noncompetitive interaction. We cannot rule out that the agonists may also interact with the orthosteric binding site, because molecular modeling studies predict that SR-17018 will bind to some of the same residues as PZM21, fentanyl, and morphine in the orthosteric pocket (41). Therefore, although it may be possible that the SR series of agonists have bitopic actions in which they can act at both an orthosteric site and a separate noncompetitive site, the data presented in this study provides strong evidence for activity

Table 2. Agonist-stimulated ^{35}S-GTPγS binding in the presence of increasing naloxone

Fig. 3 *A–C*

^{35}S-GTPγS	DAMGO		SR-17018		SR-14968		
[Naloxone]	EC_{50}, nM	%Emax	EC_{50}, nM	%Emax	EC_{50}, nM	%Emax	αβ
None	17 *(14 to 20)*	*100*	62 *(44 to 87)*	*59 (55 to 62)*	*3.9 (3.1 to 5.0)*	99 *(96 to 103)*	**0.0029**
1 nM	36 *(32 to 42)*	*shared*	217 *(149 to 317)*	*shared*	7.2 *(5.4 to 9.6)*	99 *(95 to 103)*	
10 nM	166 *(148 to 186)*	*shared*	2085 *(1397 to 3058)*	*shared*	27 *(20 to 34)*	92 *(88 to 96)*	
100 nM	1455 *(1211 to 1749)*	*shared*	12070*(8134 to 18660)*	*shared*	168 *(123 to 227)*	70 *(65 to 75)*	

Mean parameters with 95% CI are shown, n = 3, see Fig. 3. αβ is provided for the fit of the allosteric operational model for SR-14968.

Table 3. Competitive and noncompetitive interactions of opioid agonists in radioligand binding assays

Fig. 3

D–F	^{3}H-DAMGO 1 nM		^{3}H-Diprenorphine 0.5 nM			^{3}H-Naloxone 1 nM		
Competing ligand	pK_i, M	*n*	pK_i, or pK_B nM	*n*	α	pK_i, or pK_B nM	*n*	α
Naloxone	9.42 *(9.35 to 9.51)*	3	8.01*(7.92 to 8.09)*	8	–	*8.89 (8.77 to 9.01)*	3	–
DAMGO	8.72 *(8.62 to 8.81)*	*3*	*ND*		–	ND		–
Sufentanil	9.61 *(9.49 to 9.74)*	3	7.74 *(7.61 to 7.87)*	6	–	ND		–
Fentanyl	8.58 *(8.47 to 8.69)*	3	6.21 *(6.06 to 6.35)*	4	–	ND		–
SR-11501	8.58 *(8.44 to 8.73)*	3	6.15 *(6.03 to 6.27)*	5	–	ND		–
Oliceridine	8.74 *(8.61 to 8.87)*	3	7.32 *(7.17 to 7.45)*	3	–	ND		–
SR-15098	8.05 *(7.91 to 8.19)*	3	6.84 *(6.33 to 7.36)*	4	1.7	ND		–
SR-15099	8.00 *(7.87 to 8.13)*	3	7.28 *(6.72 to 7.99)*	4	1.6	ND		–
SR-17018	8.02 *(7.88 to 8.16)*	3	7.09 *(6.60 to 7.63)*	7	1.4	7.10 *(6.86 to 7.35)*	3	2.0
SR-14968	9.51 *(9.37 to 9.68)*	3	7.35 *(7.15 to 7.55)*	6	4.8	7.62 *(7.43 to 7.81)*	3	6.8

The mean parameters with 95% CI are present with the number of independent curves are shown in the table (*n*). Not determined (ND).

at an allosteric site. This is particularly evident in mouse brainstem membranes, where SR-17018 and SR-15099, although partial agonists, are unable to compete with DAMGO-stimulated GTPγS binding suggesting that, in vivo, their effect on MOR activation may be predominantly noncompetitive. Additional structural and molecular mutational studies will help to further elucidate the nature of the allosteric interaction induced by SR-17018 and SR-14968 binding to MOR. However, it remains an attractive hypothesis that selectively engaging the receptor through this sort of interaction may be a means to stabilize MOR in a G protein-coupling active state.

Previously, we showed that chronic SR-17018 (up to 48 mg/kg/day, twice a day, 6 d) does not produce tolerance in the hot plate antinociception assay (25) nor in the mouse formalin assay (18); SR-17018 also retains efficacy in a mouse chemotherapeutic-induced neuropathy model following repeated dosing (18). Interestingly, substitution of SR-17018 in morphine-tolerant mice reverses morphine tolerance while preventing abstinence-induced withdrawal (25). We hypothesize that these noncompetitive properties of SR-17018 may lead to stabilizing a G protein signaling state of the receptor and, in this manner, may facilitate restoration of orthosteric agonist (morphine) sensitivity while maintaining receptor activation (prevention of withdrawal).

The noncompetitive nature of these agonists may also be beneficial for improving naloxone sensitivity in the case of respiratory suppression. Radioligand competition data, when fit to the allosteric operational model, reveal α values greater than 1, which indicates the presence of the SR compounds increases the affinity of ^{3}H-naloxone and ^{3}H-diprenorphine for the receptor (Table 3 and Fig. 3 *E* and *F*) (44). This relationship is further supported by the naloxone competition in the GTPγS binding studies. Since naloxone produces a dose-dependent decrease in the functional response produced by SR-14968 (Fig. 3*C* and Table 2), the allosteric operational model fit of the data highlights negative activation cooperativity ($\alpha\beta < 1$, Table 2). This property would effectively make the SR-14968-bound receptor more sensitive to the action of naloxone at the orthosteric site and the experimental data demonstrating that low-dose naloxone

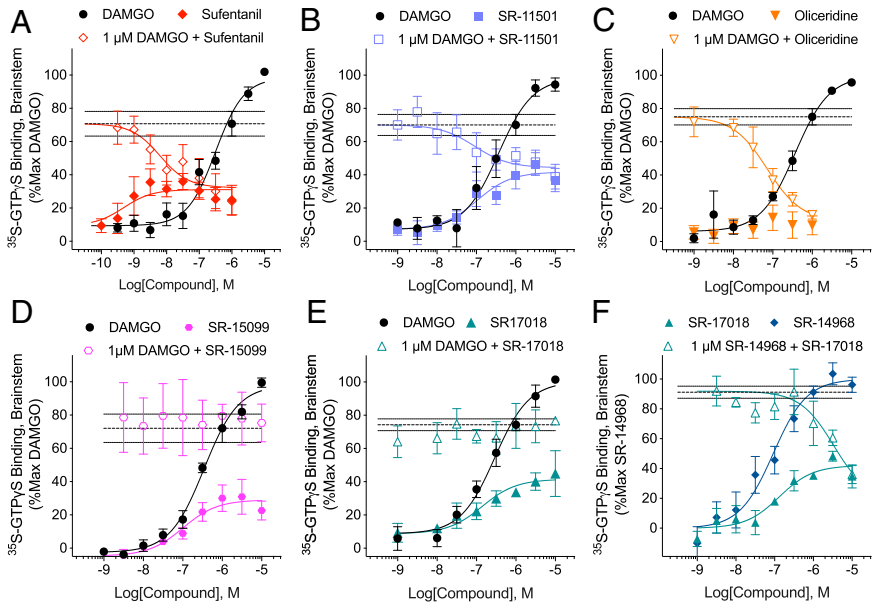

Fig. 4. The evaluation of competitive nature of partial agonists in untreated membranes from mouse brain-stem. (*A*) Sufentanil, (*B*) SR-11501, and (*C*) oliceridine compete with 1 μM DAMGO in the ^{35}S-GTPγS binding assay with oliceridine producing very little ^{35}S-GTPγS binding in mouse brainstem membranes alone. (*D*) SR-15099 and (*E*) SR-17018 are partial agonists for stimulating ^{35}S-GTPγS binding in the brain-stem but do not compete with DAMGO. (*F*) SR-14968 is a full agonist at MOR in the brain-stem relative to DAMGO (SR-14968 Emax: 1.40 ± 0.15 fold over veh, $n = 4$; DAMGO: 1.50 ± 0.02 fold over vehicle, $n = 30$), SR-17018 competes with 1 μM SR-14968. Also shown are mean with SEM. The dotted lines in each graph indicate the mean response of 1 μM DAMGO (*A–E*) or SR14968 (*F*) with SEM. See Table 4 for parameters and n values.

Table 4. ^{35}S-GTPγS binding parameters in mouse brainstem membranes

Agonist	Stimulation			+ 1μM DAMGO or SR-14968		
Fig. 4	EC_{50}, nM	% Emax*	*n*	IC_{50}, nM	% Emax*	*n*
A–E. DAMGO	240 *(188 to 305)*	100%	30	–	–	
A Sufentanil	0.48 *(0.10 to 2.24)*	31 *(26 to 37)*	5	6.0 *(1.1 to 40)*	32 *(17 to 43)*	5
B Oliceridine	NC	[10 ± 5]	7	72 *(30 to 169)*	12 *(0 to 25)*	5
C SR-11501	103 *(25 to 449)*	42 *(34 to 52)*	5	91 *(11 to 811)*	45 *(34 to 54)*	5
D SR-17018	124 *(52 to 294)*	48 *(42 to 56)*	9	NC	[78 ± 2]	4
E SR-15099	101 *(26 to 341)*	29 *(22 to 37)*	5	NC	[75 ± 11]	3
	EC_{50}, nM	% Emax†	n	IC_{50}, nM	% Emax†	n
F SR-14968	88 *(48 to 159)*	100%	4	–	–	
G SR-17018	132 *(35 to 479)*	42 *(32 to 53)*	4	NC	[36 ± 6]	4

*Percent Emax of DAMGO; bottom, shaded.
†Percent Emax of SR-14968; the means are presented with 95% CI, the number of mice is indicated (*n*), and DAMGO was included in every experiment. Competition parameters were derived by constraining the top to the average 1 μM DAMGO (or SR-14968) response obtained in each experiment. Bracketed [Emax] values represent the percent stimulation at the highest concentration tested for curves that did not converge (NC).

reversal of SR-14968-mediated respiratory suppression is in support of this proposed mechanism. This improved sensitivity of naloxone could be considered a benefit for reversing the effects of the noncompetitive agonist in cases of respiratory distress.

In this study, we do not prove that the elevation in baseline observed for SR-17018 and SR-14968 is due to or contributes to the biased agonism (GTPγS binding versus β-arrestin2 enzyme fragment complementation [EFC] assays) observed for these compounds; however, we do note that the structurally related agonist SR-11501, which does not show bias for promoting G protein signaling over β-arrestin2 recruitment (17), does not induce the elevated baseline; moreover, it fully displaces ^{3}H-diprenoprhine binding and is competitive for DAMGO stimulation in mouse brainstems. Oliceridine, which has been reported to show bias for G protein signaling (inhibition of cAMP accumulation versus β-arrestin2 EFC), also does not induce this elevation in GTPγS binding and has been reported to be an orthosteric agonist (45). These findings underscore the fact that bias determined by different cellular readouts is the product of a number of different variables collapsing into a limited number of signal readouts. In the case of SR-17018 and SR-14968, we hypothesize that the noncompetitive binding component may contribute to the measured bias between GTPγS binding and β-arrestin2 recruitment (17). However, further studies are needed to delineate these interactions.

The question remains as to whether the improved therapeutic window associated with SR-17018 observed in mice, namely, an improvement in antinociception while protecting from respiratory suppression and tolerance (17, 18, 25), is due to the bias against β-arrestin2 recruitment or due to the differences in G protein–mediated signaling observed for these ligands. The continued development of pharmacologically rich and diverse opioid ligands will aid in the delineation of the favorable and unfavorable signaling profiles in vitro that predict gains in therapeutic benefit over adverse events in vivo.

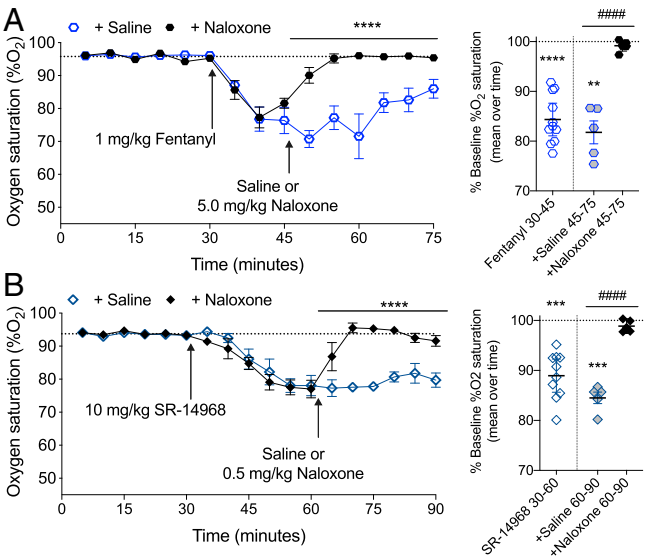

Fig. 5. Naloxone reversal of fentanyl- and SR-14968-induced respiratory suppression. (*A*) Following a 30-min habituation to determine the baseline, the mice were treated with 1 mg/kg, i.p. fentanyl; after 15 min, naloxone (5 mg/kg, i.p.) was administered; the dotted line indicates the mean baseline response over the first 30 min. Comparing the fentanyl + naloxone and fentanyl + saline effect by two-way RM-ANOVA: $F_{(1\text{-}9)}$=49.86, ****P < 0.0001, n = 5 saline, 6 naloxone. The mean of $\%O_2$ for each time bin is presented to the right comparing drug response to baseline (**P < 0.01, ****P < 0.0001, one-way RM-ANOVA) and comparing saline to naloxone ($^{\#\#\#\#}P$ < 0.0001, unpaired Student's t test). (*B*) SR-14968 (10 mg/kg, i.p.) was administered and, after 30 min, the mice were given naloxone (0.5 mg/kg, i.p.); the dotted line indicates the mean baseline response over the first 30 min. Comparing the SR-14968 + naloxone and SR-14968 + saline effect by two-way RM-ANOVA: $F_{(1\text{-}8)}$=101.6, ****P < 0.0001, n = 5 per group. The mean of $\%O_2$ for each time bin comparing drug response to the baseline (***P < 0.001, one-way RM-ANOVA) and comparing the saline to naloxone effect ($^{\#\#\#\#}P$ < 0.0001, unpaired Student's t test).

Methods

Compounds. Morphine sulfate pentahydrate were purchased from Millipore Sigma or received from the National Institute on Drug Abuse (NIDA) Drug Supply. SR-17018, SR-14968, SR-15098, SR-15099, and SR-11501 as mesylate salts were synthesized at SR as previously described and validated by NMR for purity greater than 95% (17). Oliceridine (TRV-130) was purchased from Cayman Chemical. Fentanyl HCl, Naloxone HCl, and DAMGO were obtained from Millipore Sigma. CTOP (the cyclized peptide: [D-Phe-Cys-Tyr-D-Trp-Orn-Thr-Pen-Thr-NH_2]) was purchased from Tocris. Compounds were prepared as 10 mM stocks in 100% DMSO (Thermo Fisher) and stored at −20 °C in 10 μL aliquots to avoid repeated freeze–thaw cycles. SR compounds are difficult to solubilize; therefore, extra care was taken with the DMSO used in preparing the stocks. Since DMSO is very hygroscopic, pure DMSO was aliquoted in glass bottles and kept at 4 °C prior to use (at 4 °C, pure DMSO should be solid). Radioligands were purchased from PerkinElmer: Guanosine triphosphate, labeled on the gamma phosphate group with ^{35}S (^{35}S-GTPγS, 1250 μCi); Naloxone, [*N*-allyl-2,3,-^{3}H] (^{3}H-Naloxone, 250 μCi; specific activity: 70, Ci/mmol); DAMGO, [Tyrosyl-3,5-^{3}H(N)], (^{3}H-DAMGO: 250 μCi; specific activity: 53.7 Ci/mmol); and Diprenorphine [15,16-^{3}H], (^{3}H-Diprenorphine, specific activity: 37 Ci/mmol).

Animals. Male C57BL6/J mice at 10 to 16 wk of age from Jackson Labs were kept on a 12-h light–dark cycle and had ad libitum access to standard rodent chow and water. All studies were performed using mice that had not been used for any other purposes. The mice were used in accordance with the National

Institutes of Health Guidelines for the Care and Use of Laboratory Animals with the approval by The SR Institute Animal Care and Use Committee.

Cell Culture. CHO-K1 (American Type Culture Collection [ATCC]) cells expressing the human MOR (CHO–MOR) were grown under Geneticin selection (500 μg/μL) in DMEM/F12 media containing 10% fetal bovine serum (FBS) as described (17, 40). Untransfected CHO-K1 cells were grown in the same manner but without Geneticin. CHO-K1 expressing haemagluttinin-tagged mouse MOR (CHO-HA-mMOR) cells were grown with 1ug/mL puromycin (17). SHSY-5Y cells were purchased from ATCC and cultured DMEM/F12 supplemented with 1x GlutaMAX (200 mM L-alanyl-L-glutamine dipeptide in 0.85% NaCl by Gibco sold as 100X stock) and 10% FBS. Cells were incubated in serum free media for timepoints as indicated in the presence of vehicle (1% DMSO) or specified compounds at the noted concentrations. Cells were then rinsed on the plate with phosphate buffered saline (PBS), dissociated with 5 mM ethylenediaminetetraacetic acid (EDTA), and then collected and pelleted in a 15-mL Falcon tube by centrifugation at 2,000 × g for 2 min; washes were repeated in PBS five times. Cell pellets were stored at −80 °C until use in the binding assays.

GTPγS Binding Assays.

No pretreatment. Assays were performed as previously described (17). The cells (MOR–CHO and SH-SY5Y cells) were serum starved for 2 h, collected in PBS with 5mM EDTA, centrifuged (2,000 rpm), and stored at −80 °C. The cells were then disrupted by Teflon-on-glass homogenization in a buffer comprised of 10 mM Tris HCl, pH 7.4, and 1 mM EDTA. The homogenates were centrifuged at 4 °C at 20,000 × g for 30 min to prepare a membrane pellet. The pellet was resuspended in ^{35}S-GTPγS binding buffer (10 mM Tris HCl, pH 7.4, 5 mM $MgCl_2$, 1 mM EDTA, 20 μM guanosine diphosphate [GDP], and 100 mM NaCl) and 0.1 nM ^{35}S-GTPγS and plated at 10 μg protein/well.

Intact cell pretreatment. For intact cell pretreatment studies, adherent cells were incubated in serum free media up to 2 h in the presence of vehicles or drugs at the concentrations and times indicated (Fig. 1). The cells were collected, centrifuged (2,000 rpm), and the pellet resuspended and centrifuged five times prior to freezing (−80 °C). The membranes were prepared and the assay performed as described for the "no pretreatment" GTPγS assays.

Cell membrane pretreatment. Untreated cells were collected and the membranes were prepared from pellets as described for the no pretreatment GTPγS binding assays (without extra wash steps). The pellet was resuspended in ^{35}S-GTPγS binding buffer (10 mM Tris HCl, pH 7.4, 5 mM $MgCl_2$, 1 mM EDTA, and 100 mM NaCl) and divided into portions for pretreatment with agonist or vehicle. Following pretreatment, membranes were centrifugated at 20,000 × *g* 4 °C for 10 min and resuspended in the same buffer; this was repeated for five washes. The final pellet was resuspended in ^{35}S-GTPγS binding buffer including 20 μM GDP plated at 10 μg protein/well in the presence of 0.1 nM ^{35}S-GTPγS for the assay (Fig. 2). In studies in which NaCl was added (Fig. 2*F*), membranes were resuspended in the GTPγS binding buffer in the absence of NaCl such that no NaCl was present during the pretreatment period; NaCl was added at the concentrations indicated at the point of including ^{35}S-GTPγS.

Mouse brainstem membranes. Brainstem membranes were prepared following homogenization as previously described (17, 46) and subject to membrane pretreatment followed by five washes (Fig. 2*H*) or assessed directly without pretreatment and extended washes (Fig. 4). In the brainstem pretreatment studies, vehicle pretreatment was assessed for each brainstem in parallel to each drug tested; in the competition studies, DAMGO was assessed in parallel for each drug in each brainstem. One brainstem = 1 mouse = 1 n.

For all experiments, protein was quantitated using the BioRad Bradford kit. In each reaction, 1% DMSO served as the vehicle. In cases in which antagonists are included, the antagonist is added during the ^{35}S-GTPγS binding incubation. Incubation was for 1 h at room temperature, and the reaction was stopped by rapid filtration onto GF/B fiberglass filter plates using a Brandel 96-well plate harvester with subsequent washes with cold dH_2O. Radioactivity was counted with Microscint on a TopCount NXT Scintillation Counter (PerkinElmer).

Homogeneous Time Resolved Fluorescence cAMP Measures. CHO–MOR cells were serum starved for 2 h in the presence of vehicle, morphine, or SR-17018 prior to collection as previously described (17). Cells were collected in PBS with 5mM EDTA, gently washed three times in PBS, and then dispersed into a 384-well plate at 5,000 cells per well. Cells were incubated in the absence of serum for 3 h prior to addition of forskolin (32 μM). Levels of cAMP were determined with the Homogenous Time-Resolved Fluorescence resonance energy transfer cAMP HiRange kit by Cisbio according to the manufacturer's instructions (Cisbio-62 AM6PEC) upon 1 h incubation with detection reagents as previously described (17). A cAMP standard curve was included in each assay to determine the concentration of cAMP generated. In the absence of forskolin, the levels of cAMP did not differ between the pretreatment groups: Veh: 0.272 ± 0.098 nM, Morphine: 0.205 ± 0.078 nM, and SR-17018: 0.150 ± 0.054 nM cAMP, $P > 0.05$, paired Student's *t* test $n = 3$ with SEM.

Radioligand Binding Assays.

Intact cell binding. CHO–MOR cells, 250,000 per well, were plated on 24-well plates and grown overnight. The following day, the cells were serum starved for 1 h with vehicle or 10 uM agonist and washed five times with PBS + 1mM $CaCl_2$ + 1mM $MgCl_2$. Following washes, all cells were incubated in PBS + 1mM $CaCl_2$ + 1mM $MgCl_2$ with 4nM [^{3}H]Naloxone for 30 min at room temperature. Nonspecific binding was determined by including 10uM naloxone. The cells were rinsed twice with ice cold PBS + 1mM CaCl2 + 1mM MgCl2 and lysed with 10% sodium dodecyl sulfate. Radioactivity was quantitated with Safety-Solve on a Beckman LS6500 liquid scintillation counter.

Pretreatment of membranes. Membranes of untreated cells were prepared as described in *GTPγS Binding Assay*; agonists or vehicle was added for 30 min (Fig. 2*C*) followed by five washes and resuspension of membranes. The determination of specific binding was determined with 3.5 to 4 nM ^{3}H-Naloxone (with 1 μM naloxone to determine nonspecific) using 20 μg protein.

Cell membrane binding. Competition binding assays (Fig. 3 *D–F*) in untreated cell membranes and cells were homogenized on ice by Teflon-on-glass dounce homogenization in homogenization buffer (50 mM Tris HCl, pH 7.4, 1 mM EDTA ± 100 mM NaCl as indicated) and pelleted by centrifugation at 4 °C at 20,000 × *g* for 30 min. The pellet was washed, pelleted, and then resuspended in radioligand assay buffer (10 mM Tris HCl, pH 7.4, 100 mM NaCl). The affinity of the radioligands used were determined in CHO–MOR cell membranes by homologous competition (^{3}H-DAMGO: K_D= 1.9 nM; ^{3}H-Naloxone: K_D = 1.2 nM) (Table 3) or by saturation binding (^{3}H-Diprenorphine: K_D = 0.78 nM) during which 10 μM naloxone was used to define nonspecific binding. For competition studies, ∼1 nM ^{3}H-DAMGO, ∼1 nM ^{3}H-Naloxone, and ∼0.5 nM ^{3}H- diprenorphine were used; 1 μM cold naloxone defined nonspecific binding in the competition assays. All radioligand binding assays were performed in 96-well plates with 20 μg protein/well, collected using a 96-well Brandel Cell Harvester followed by several washes with cold 10mM Tris (pH 7.4), and counted on a TopCount NXT Scintillation Counter (PerkinElmer) with 2.7-fold efficiency correction for converting CPM to disintegrations per minute. Competitive radioligand binding studies were analyzed using the heterologous competition equation built into GraphPad Prism. The data presented for ^{3}H-DAMGO binding were published previously for some of the agonists as the mean of the individual K_i per replicates; here, all affinity values are presented as the K_i derived from the combined curves with 95% CI (17).

Respiratory suppression. Measures of $\%O_2$ arterial oxygen saturation were recorded using the MouseOx Plus pulse oximeter as previously described (17). Mice were shaved around the neck and were habituated for approximately an hour to the pulse oximetry collars and modified conical tubes (for mild restraint) for 2 d prior to drug treatment and measurements. Baseline recordings were made 30 min immediately prior to drug treatment. Mice were administered SR-14968 (10 mg/kg, i.p. based on base weight) prepared in vehicle (1:1:8 of DMSO, Tween80, water) or fentanyl HCl (1 mg/kg, i.p. based on salt weight) prepared in saline. Naloxone HCl was prepared in saline for 0.5 or 5 mg/kg i.p. dosing (based on salt weight). All compounds were dosed at 10 μL per gram mouse body weight at time of injection. The experimenter was blinded to the naloxone and saline treatment. A total of 22 mice were used, and one animal was eliminated based on the criterion that the baseline $\%O_2$ must be above 92%.

Data Analysis.

^{35}S-GTP binding following drug pretreatment. Since ^{35}S-GTPγS is subject to rapid radioactive decay, experiments that were performed in parallel with corresponding vehicle-treated groups are presented within the same graphs and the CPM radioactivity measures are provided. A vehicle pretreatment was included for each drug treatment day; however, not all drugs were tested in every experiment. Therefore, statistical comparisons are made by paired Student's *t* test comparing vehicle and drug effect for each experimental replicate. We employed ratio paired Student's *t* tests as we anticipated a more consistent fold change rather than a subtractive change (due to the variation in basal radioactivity measures following vehicle pretreatment). Exceptions arise when all drugs are included in the same experiment with one vehicle, at which point a one-way repeated measures (RM)-ANOVA is applied with a Dunnett's post hoc test to compare drug effect to vehicle pretreatment.

Nonlinear regression. EC_{50} and Emax values were calculated from concentration response curves by fitting to a three-parameter nonlinear regression using GraphPad Prism 9.0. In the Schild analysis, EC_{50} values for each curve were plotted as a function of Log(DR-1) in which DR is the EC_{50} shift produced in the presence of each concentration of the competing ligand. In all cases, the parameters presented in the tables are from the curves presented in the figures. For changes in EC_{50} and Emax, an unpaired Student's *t* test was used. In some cases, data are

PHARMACOLOGY

presented as the percent of the DAMGO stimulation after vehicle subtraction in which both the DAMGO points and the vehicles were included on the same plate; these cases are indicated within the legends. To describe allosteric interactions, pK_B and α values were calculated when the lower CI of the bottom fit of the curve was greater than 0. When necessary to analyze noncompetitive radioligand binding inhibition, the curves were fit to the equation (47)

$$Y = B_{\text{Max}} * \frac{A}{A + \left(K * \left(\frac{K_X + X}{K_X + \frac{X}{\alpha}}\right)\right)},$$

in which B_{Max} is the maximum binding of the system, A and K represent the concentration and affinity values of the radioligand, X = concentration of each test compound, K_X = test compounds affinity constant, and α defines the binding cooperativity between the two ligands at their respective sites.

Individual statistical analyses are indicated within the figure legends; GraphPad Prism software (versions 8.0 and 9.0) was used for all plotting and statistical analyses.

The allosteric operational model (48) was used to determine the $\alpha\beta$ cooperativity value for the combined inhibitory effect of naloxone on SR-14968 mediated response

$$\text{Response} = \frac{\text{Emax} \cdot (\tau_A[A](K_B + \alpha\beta[B]) + \tau_B[B]K_A)^n}{([A]K_B + K_AK_B + K_A[B] + \alpha[A][B])^n + (\tau_A[A](K_B + \alpha\beta[B]) + \tau_B[B]K_A)^n},$$

in which Emax is the maximum response of the system, τ_A and τ_B describe the efficacy, and K_A and K_B describe the affinity of the allosteric [A] and orthosteric [B] ligands, respectively. n is the system transducer slope, α describes the binding cooperativity, and $\alpha\beta$ describe the composite product of the binding and activation cooperativity. For the fit of the data, the α and K_B (for naloxone) values produced in ^{3}H-naloxone binding experiments were used for the fit. All parameters except $\alpha\beta$ were either defined as constants or shared between the fit of all data.

Mouse respiratory studies. For the in vivo studies, two-way RM-ANOVA were performed over time with difference assessed only following naloxone or saline treatment. The mean effects of each phase (opioid agonist, saline, and naloxone treatment) are compared to the baseline by one-way RM-ANOVA; the means of saline versus naloxone rescue of drug effects are compared by unpaired Student's *t* test.

Data Availability. All study data are included in the article and/or *SI Appendix*.

ACKNOWLEDGMENTS This work has been funded by the National Institutes on Drug Abuse Grants NIH R01DA038964 (L.M.B.), R01DA033073 (L.M.B., T.D.B.), and F32DA052124 (A.A.-C.). We thank Vuong Dang for technical assistance and Gogce Crynen, PhD, for consulting on statistical analysis.

1. G. W. Pasternak, Mu opioid pharmacology: 40 years to the promised land. *Adv. Pharmacol.* **82**, 261–291 (2018).
2. J. T. Williams *et al.*, Regulation of μ-opioid receptors: Desensitization, phosphorylation, internalization, and tolerance. *Pharmacol. Rev.* **65**, 223–254 (2013).
3. J. T. Williams, Desensitization of functional μ-opioid receptors increases agonist off-rate. *Mol. Pharmacol.* **86**, 52–61 (2014).
4. S. Schulz *et al.*, Morphine induces terminal micro-opioid receptor desensitization by sustained phosphorylation of serine-375. *EMBO J.* **23**, 3282–3289 (2004).
5. J. P. Celver, J. Lowe, A. Kovoor, V. V. Gurevich, C. Chavkin, Threonine 180 is required for G-protein-coupled receptor kinase 3- and beta-arrestin 2-mediated desensitization of the mu-opioid receptor in Xenopus oocytes. *J. Biol. Chem.* **276**, 4894–4900 (2001).
6. G. W. Terman *et al.*, G-protein receptor kinase 3 (GRK3) influences opioid analgesic tolerance but not opioid withdrawal. *Br. J. Pharmacol.* **141**, 55–64 (2004).
7. K. M. Raehal, L. M. Bohn, The role of beta-arrestin2 in the severity of antinociceptive tolerance and physical dependence induced by different opioid pain therapeutics. *Neuropharmacology* **60**, 58–65 (2011).
8. A. Kliewer *et al.*, Phosphorylation-deficient G-protein-biased μ-opioid receptors improve analgesia and diminish tolerance but worsen opioid side effects. *Nat. Commun.* **10**, 367 (2019).
9. L. M. Bohn, R. R. Gainetdinov, F. T. Lin, R. J. Lefkowitz, M. G. Caron, Mu-opioid receptor desensitization by beta-arrestin-2 determines morphine tolerance but not dependence. *Nature* **408**, 720–723 (2000).
10. E. J. Whalen, S. Rajagopal, R. J. Lefkowitz, Therapeutic potential of β-arrestin- and G protein-biased agonists. *Trends Mol. Med.* **17**, 126–139 (2011).
11. P. W. de Waal *et al.*, Molecular mechanisms of fentanyl mediated β-arrestin biased signaling. *PLOS Comput. Biol.* **16**, e1007394 (2020).
12. K. J. Gregory, P. M. Sexton, A. B. Tobin, A. Christopoulos, Stimulus bias provides evidence for conformational constraints in the structure of a G protein-coupled receptor. *J. Biol. Chem.* **287**, 37066–37077 (2012).
13. L. M. Luttrell, S. Maudsley, L. M. Bohn, Fulfilling the promise of "biased" G protein-coupled receptor agonism. *Mol. Pharmacol.* **88**, 579–588 (2015).
14. R. B. Mailman, GPCR functional selectivity has therapeutic impact. *Trends Pharmacol. Sci.* **28**, 390–396 (2007).
15. J. D. Urban *et al.*, Functional selectivity and classical concepts of quantitative pharmacology. *J. Pharmacol. Exp. Ther.* **320**, 1–13 (2007).
16. L. M. Wingler *et al.*, Angiotensin analogs with divergent bias stabilize distinct receptor conformations. *Cell* **176**, 468–478.e11 (2019).
17. C. L. Schmid *et al.*, Bias factor and therapeutic window correlate to predict safer opioid analgesics. *Cell* **171**, 1165–1175.e13 (2017).
18. F. Pantouli *et al.*, Comparison of morphine, oxycodone and the biased MOR agonist SR-17018 for tolerance and efficacy in mouse models of pain. *Neuropharmacology* **185**, 108439 (2021).
19. K. M. Raehal, C. L. Schmid, C. E. Groer, L. M. Bohn, Functional selectivity at the μ-opioid receptor: Implications for understanding opioid analgesia and tolerance. *Pharmacol. Rev.* **63**, 1001–1019 (2011).
20. L. M. Bohn, R. J. Lefkowitz, M. G. Caron, Differential mechanisms of morphine antinociceptive tolerance revealed in (beta)arrestin-2 knock-out mice. *J. Neurosci.* **22**, 10494–10500 (2002).
21. M. Connor, E. E. Bagley, B. C. Chieng, M. J. Christie, β-arrestin-2 knockout prevents development of cellular μ-opioid receptor tolerance but does not affect opioid-withdrawal-related adaptations in single PAG neurons. *Br. J. Pharmacol.* **172**, 492–500 (2015).
22. D. Wang *et al.*, Basal signaling activity of mu opioid receptor in mouse brain: Role in narcotic dependence. *J. Pharmacol. Exp. Ther.* **308**, 512–520 (2004).
23. L. J. Sim-Selley *et al.*, Region-dependent attenuation of mu opioid receptor-mediated G-protein activation in mouse CNS as a function of morphine tolerance. *Br. J. Pharmacol.* **151**, 1324–1333 (2007).
24. D. E. Selley, L. J. Sim, R. Xiao, Q. Liu, S. R. Childers, mu-opioid receptor-stimulated guanosine-5'-O-(gamma-thio)-triphosphate binding in rat thalamus and cultured cell lines: Signal transduction mechanisms underlying agonist efficacy. *Mol. Pharmacol.* **51**, 87–96 (1997).
25. T. W. Grim *et al.*, A G protein signaling-biased agonist at the μ-opioid receptor reverses morphine tolerance while preventing morphine withdrawal. *Neuropsychopharmacology* **45**, 416–425 (2020).
26. S. K. Sharma, W. A. Klee, M. Nirenberg, Opiate-dependent modulation of adenylate cyclase. *Proc. Natl. Acad. Sci. U.S.A.* **74**, 3365–3369 (1977).
27. T. Avidor-Reiss *et al.*, Adenylylcyclase supersensitization in mu-opioid receptor-transfected Chinese hamster ovary cells following chronic opioid treatment. *J. Biol. Chem.* **270**, 29732–29738 (1995).
28. P. A. Zaki, D. E. Keith Jr., G. A. Brine, F. I. Carroll, C. J. Evans, Ligand-induced changes in surface mu-opioid receptor number: Relationship to G protein activation? *J. Pharmacol. Exp. Ther.* **292**, 1127–1134 (2000).
29. B. Frances, C. Moisand, J. C. Meunier, Na+ ions and Gpp(NH)p selectively inhibit agonist interactions at mu- and kappa-opioid receptor sites in rabbit and guinea-pig cerebellum membranes. *Eur. J. Pharmacol.* **117**, 223–232 (1985).
30. P. Jauzac, B. Frances, A. Puget, C. Moisand, J. C. Meunier, Differential regulation of two molecular forms of a mu-opioid receptor type by sodium ions, manganese ions and by guanyl-5'-yl imidodiphosphate. *J. Recept. Res.* **6**, 1–25 (1986).
31. G. W. Pasternak, S. H. Snyder, Identification of novel high affinity opiate receptor binding in rat brain. *Nature* **253**, 563–565 (1975).
32. C. B. Pert, G. Pasternak, S. H. Snyder, Opiate agonists and antagonists discriminated by receptor binding in brain. *Science* **182**, 1359–1361 (1973).
33. Y. Shang *et al.*, Mechanistic insights into the allosteric modulation of opioid receptors by sodium ions. *Biochemistry* **53**, 5140–5149 (2014).
34. S. Ott, T. Costa, A. Herz, Sodium modulates opioid receptors through a membrane component different from G-proteins. Demonstration by target size analysis. *J. Biol. Chem.* **263**, 10524–10533 (1988).
35. T. Costa, J. Lang, C. Gless, A. Herz, Spontaneous association between opioid receptors and GTP-binding regulatory proteins in native membranes: Specific regulation by antagonists and sodium ions. *Mol. Pharmacol.* **37**, 383–394 (1990).
36. E. L. Stahl, L. Zhou, F. J. Ehlert, L. M. Bohn, A novel method for analyzing extremely biased agonism at G protein-coupled receptors. *Mol. Pharmacol.* **87**, 866–877 (2015).
37. R. Hill, R. Santhakumar, W. Dewey, E. Kelly, G. Henderson, Fentanyl depression of respiration: Comparison with heroin and morphine. *Br. J. Pharmacol.* **177**, 254–266 (2020).
38. G. Vauquelin, S. Bostoen, P. Vanderheyden, P. Seeman, Clozapine, atypical antipsychotics, and the benefits of fast-off D2 dopamine receptor antagonism. *Naunyn Schmiedebergs Arch. Pharmacol.* **385**, 337–372 (2012).
39. C. E. Groer *et al.*, An opioid agonist that does not induce mu-opioid receptor–Arrestin interactions or receptor internalization. *Mol. Pharmacol.* **71**, 549–557 (2007).
40. H. Xu *et al.*, A comparison of noninternalizing (herkinorin) and internalizing (DAMGO) mu-opioid agonists on cellular markers related to opioid tolerance and dependence. *Synapse* **61**, 166–175 (2007).

41. S. Podlewska, R. Bugno, L. Kudla, A. J. Bojarski, R. Przewlocki, Molecular modeling of μ opioid receptor ligands with various functional properties: PZM21, SR-17018, morphine, and fentanyl-simulated interaction patterns confronted with experimental data. *Molecules* **25**, 4636 (2020).
42. W. Huang *et al.*, Structural insights into μ-opioid receptor activation. *Nature* **524**, 315–321 (2015).
43. A. Manglik *et al.*, Crystal structure of the μ-opioid receptor bound to a morphinan antagonist. *Nature* **485**, 321–326 (2012).
44. T. Kenakin, Allosteric theory: Taking therapeutic advantage of the malleable nature of GPCRs. *Curr. Neuropharmacol.* **5**, 149–156 (2007).
45. S. M. DeWire *et al.*, A G protein-biased ligand at the μ-opioid receptor is potently analgesic with reduced gastrointestinal and respiratory dysfunction compared with morphine. *J. Pharmacol. Exp. Ther.* **344**, 708–717 (2013).
46. T. W. Grim, A. Acevedo-Canabal, L. M. Bohn, Toward directing opioid receptor signaling to refine opioid therapeutics. *Biol. Psychiatry* **87**, 15–21 (2020).
47. F. J. Ehlert, Estimation of the affinities of allosteric ligands using radioligand binding and pharmacological null methods. *Mol. Pharmacol.* **33**, 187–194 (1988).
48. C. Valant, C. C. Felder, P. M. Sexton, A. Christopoulos, Probe dependence in the allosteric modulation of a G protein-coupled receptor: Implications for detection and validation of allosteric ligand effects. *Mol. Pharmacol.* **81**, 41–52 (2012).